

# Nogo-A promotes inflammatory heat hyperalgesia by maintaining TRPV-1 function in the rat dorsal root ganglion neuron

Fang Hu,<sup>\*,†,1</sup> Huai-Cun Liu,<sup>‡,1</sup> Dong-Qiang Su,<sup>‡,1</sup> Hai-Jing Chen,<sup>\*</sup> Sun-On Chan,<sup>§</sup> Yun Wang,<sup>\*,¶,2</sup> and Jun Wang<sup>‡,3</sup>

<sup>\*</sup>Department of Neurobiology, Neuroscience Research Institute, Key Laboratory for Neuroscience of Ministry of Education and Neuroscience, National Health Commission, Peking University Health Science Center, Beijing, China; <sup>†</sup>Department of Pharmacology, Qingdao University School of Pharmacy, Qingdao, China; <sup>‡</sup>Department of Anatomy and Histology, School of Basic Medical Sciences, Peking University, Beijing, China; <sup>§</sup>School of Biomedical Sciences, Faculty of Medicine, The Chinese University of Hong Kong, Hong Kong, China; and <sup>¶</sup>Peking University–International Data Group (PKU-IDG)/McGovern Institute for Brain Research, Peking University, Beijing, China

**ABSTRACT:** Nogo-A is a key inhibitory molecule of axon regeneration in oligodendrocytes. However, little is known about its role in adult neurons. In this study, we showed an important function of Nogo-A on regulation of inflammatory pain in dorsal root ganglion (DRG) neurons. In adult rats with complete Freund's adjuvant (CFA) hind paw inflammation, DRG neurons showed a significant increase in Nogo-A expression. Disruption of Nogo-A signaling with Nogo-66 receptor antagonist peptide, Nogo-A blocking antibody, Nogo-A short hairpin RNA, or Nogo-A gene knockout attenuated CFA-induced inflammatory heat hyperalgesia. Moreover, disruption of Nogo-A signaling suppressed the function and expression in DRG neurons of the transient receptor potential vanilloid subfamily member (TRPV)-1 channel, which is known to be the endogenous transducer of noxious heat during inflammation. These effects were accompanied with a reduction in LIM domain kinase (LIMK)/cofilin phosphorylation and actin polymerization. Similar disruption of actin filament architecture by direct action of Latrunculin A reduced the TRPV-1 activity and up-regulation of TRPV-1 protein caused by CFA. We conclude that Nogo-A plays an essential role in the development of inflammatory heat hyperalgesia, partly through maintaining TRPV-1 function *via* activation of the LIMK/cofilin pathway, which regulates actin filament dynamics. These findings support a therapeutic potential of modulating Nogo-A signaling in pain management.—Hu, F., Liu, H.-C., Su, D.-Q., Chen, H.-J., Chan, S.-O., Wang, Y., Wang, J. Nogo-A promotes inflammatory heat hyperalgesia by maintaining TRPV-1 function in the rat dorsal root ganglion neuron. *FASEB J.* 33, 668–682 (2019). [www.fasebj.org](http://www.fasebj.org)

**KEY WORDS:** RTN4A · inflammatory pain · cytoskeleton

Chronic pain associated with injury or disease is caused by activation of nociceptors in the skin and soft tissues during inflammation. Inflammatory soup can generate robust hypersensitivity to heat in nociceptive neurons within the

dorsal root ganglia (DRGs). The transient receptor potential vanilloid subfamily member (TRPV)-1 channel is a key element underlying the generation of inflammatory heat hyperalgesia (1–3) and is the major target for development of novel analgesics (3, 4). Some molecules act directly on the TRPV-1 channel in primary afferents as positive allosteric modulators, whereas others bind to their own receptors and modulate TRPV-1 through the downstream intracellular signaling pathway (5). The search for novel modulators of TRPV-1 has drawn much attention to the design of new analgesic drugs with fewer side effects (6).

Nogo-A is one of the 3 major alternatively spliced isoforms (Nogo-A, -B and -C) of the reticulon 4 (*RTN4*; also known as *NOGO*) gene and is the major isoform in the adult nervous system (7, 8). It is restricted mainly to oligodendrocytes in postnatal and adult CNS tissues (9, 10) and works as one of the key myelin-associated inhibitory molecules to axon regeneration (7, 8, 11, 12). However, its function in neurons has not been fully resolved. During development

**ABBREVIATIONS:** CFA, complete Freund's adjuvant; DRG, dorsal root ganglion; F-actin, filamentous actin; G-actin, globular actin; GFP, green fluorescent protein; gRNA, guide RNA; Het, heterozygous; KO, knockout; Lat, latrunculin; S1PR, sphingosine 1-phosphate receptor; shRNA, short hairpin RNA; TRITC, tetramethylrhodamine; TRPV, transient receptor potential vanilloid subfamily member; WT, wild type

<sup>1</sup> These authors contributed equally to this work.

<sup>2</sup> Correspondence: Department of Neurobiology, Neuroscience Research Institute, Peking University, School of Basic Medical Sciences, Peking University, Beijing 100083, China. E-mail: wangy66@bjmu.edu.cn

<sup>3</sup> Correspondence: Department of Anatomy and Histology, School of Basic Medical Sciences, Peking University, No. 38 Xueyuan Rd., Haidian District, Beijing 100083, China. E-mail: wangjun74008@bjmu.edu.cn

doi: 10.1096/fj.201800382RR

This article includes supplemental data. Please visit <http://www.fasebj.org> to obtain this information.

of the brain, Nogo-A is extensively expressed in different types of neurons and plays diverse roles in neuronal migration (13, 14), neurite outgrowth, axon guidance (15, 16), and myelin formation (17, 18). The neuronal expression of Nogo-A in central and peripheral neurons gradually decreases to low or undetectable levels after birth. However, a few neuron types retain high levels of Nogo-A expression, including those in the olfactory bulb, hippocampus, motor horn of the spinal cord, and DRGs (9, 19). Its function in adult neurons, particularly in DRGs, is largely unknown.

The topologies and downstream pathways of Nogo-A have not been fully revealed. Nogo-A is mainly localized in the endoplasmic reticulum, but some is present on the cell surface (20). The N terminus, exon 3 sequence, and Nogo-66 domain of the C terminus have been found on the extracellular surface and work as functional domains (19–21). The 2 well-studied functional regions are Nogo-66 and Nogo- $\Delta$ 20 (aa 544–725 of rat Nogo-A) (20, 22). Both can activate the small GTPase RhoA, LIM domain kinase (LIMK)-1, and actin depolymerization factor cofilin *via* the Nogo-66 receptor (NgR) and sphingosine 1-phosphate receptor (S1PR)-2 (19, 23–25). It has been reported by our laboratory that the LIMK-dependent actin polymerization in DRGs is necessary for the development of inflammatory pain (26). As an actin modulator, Nogo-A may serve as an upstream molecule of the LIMK/cofilin pathway and modulate the function of TRPV-1 in inflammatory pain.

In this study, we determined whether Nogo-A plays a role in modulating pain transmission in adult rats. We report that Nogo-A in DRG neurons promoted the development of inflammatory heat hyperalgesia induced by complete Freund's adjuvant (CFA). Furthermore, Nogo-A signaling was necessary to trigger the dramatic up-regulation of TRPV-1 protein and maintained its function in inflammatory pain. This regulation was achieved partly by activation of the LIMK/cofilin pathway, which regulates actin dynamics, supporting a crucial role for Nogo-A in pain modulation.

## MATERIALS AND METHODS

### Animals

Male Sprague-Dawley rats weighing 200–220 g were supplied by the Animal Center of Peking University Health Science Center. The animals were housed in climate-controlled rooms on a 12-h light–dark cycle (lights on 8 AM) with free access to food and water. All experimental procedures were approved by the Animal Care and Use Committee of Peking University, and efforts were made to minimize the discomfort of the animals.

The Nogo-A (*Rtn4*)-knockout (KO) rats were generated in Nanjing Biomedical Research Institute of Nanjing University (Nanjing, China). The transcript of Nogo-A (*Rtn4*)-201 is selected for generation of KO animals. Nogo-A (*Rtn4*)-KO rats were generated by using the clustered regularly interspaced short palindromic repeats (CRISPR)/CRISPR-associated (Cas) 9 system. Guide (g)RNAs direct Cas9 endonuclease cleavage of the Nogo-A (*Rtn4*) gene and create a double-strand break. Such breaks will be repaired and result in a frame shift from exon 1. Two suitable gRNAs have been found on exon 3 of Nogo-A (*Rtn4*)-201: Nogo-A-S1: 5'-CCAGGTAACACTGTTT-CGCTGG-3'; and Nogo-A-S2: 5'-ACACTGCTGATAAGTT-ACCAAGG-3'.

### Induction of inflammatory pain

To induce inflammatory pain, 100  $\mu$ l 25% CFA (F5881; MilliporeSigma, Burlington, MA, USA) was injected into the plantar surface of the left hind paw in adult rats under brief isopentane anesthesia. CFA (100%) was diluted to 25% in incomplete Freund's adjuvant (F5506; MilliporeSigma) to avoid excessive inflammation and spontaneous pain behavior. CFA injection produces local swelling characterized by erythema, edema, and hypersensitivity. The animals continued to exhibit normal grooming behavior and weight gain over the course of the experiments (27).

### Intrathecal injection of calpain inhibitors, peptides, antibodies, or short hairpin RNA

Implantation of intrathecal cannulae was performed as described by Størkson *et al.* (28). Rats were anesthetized with 10% chloral hydrate (0.3 g/kg, i.p.). The back skin was incised to expose the vertebral column. The intraspinal space between lumbar vertebrae 4 and 5 (L4–L5) was chosen as the site for insertion of the needle. The correct intrathecal location was confirmed by tail flick or a paw retraction. Polyethylene (PE)-10 catheters (outer diameter, 0.61 mm) were implanted with a catheter-through-needle technique to reach the lumbar enlargement of the spinal cord. The outer end of the catheter was plugged and fixed to the skin upon closure of the wound. The rats were individually housed after surgery and allowed to recover. Animals showing motor impairment after intrathecal cannula placement were excluded from the study.

Five days after the surgery, Nogo-A short hairpin RNA (shRNA), the NgR antagonist peptide (NEP 1-40), the S1PR2 antagonist JTE-013, or blocking antibody was infused into the intraspinal space to suppress Nogo-A signaling in the DRG neurons. NEP 1-40 and the scrambled control were synthesized and purified by the Chinese Peptide Co. (Shanghai, China). The sequences of NEP 1-40 and the control scrambled peptide were RIYKGVIIQAIQKSDEGHPFRAYLESEVAISEELVQKYSNS and DERSGVKQVERIGKYNELYASEQSPIAEISIAHKQSVLF, respectively (29). The peptides were dissolved in saline to a final concentration of 1  $\mu$ g/ $\mu$ l and were injected *via* catheter in a volume of 3, 10, or 30  $\mu$ l, followed by 10  $\mu$ l saline for flushing, over a period of 3–5 min. JTE-013 (0.1, 1.0, or 10  $\mu$ g; Tocris Bioscience, Bristol, United Kingdom) was intrathecally injected to block the function of receptor of Nogo- $\Delta$ 20–S1PR2. After the injection, the needle remained *in situ* for 2 min before it was withdrawn. For administration of the calpain inhibitors, calpeptin (10  $\mu$ l and 20 mM) or MDL28170 (10 and 2.5  $\mu$ g/ $\mu$ l) (both from MilliporeSigma) was injected intrathecally 30 min before peptide injection. In other animals, Nogo-A antibody (sc-11032) or normal goat IgG (sc-2028) (both from Santa Cruz Biotechnology, Dallas, TX, USA), prepared in a concentration of 0.2  $\mu$ g/ $\mu$ l, was injected intrathecally in a volume of 1, 3, or 10  $\mu$ l. A half hour after the injection of peptide or antibody, 25% CFA was injected. Nociceptive responses were measured 1, 2, 6, and 24 h after administration of CFA.

The shRNA plasmids were generated by Syngentech (Beijing, China). Oligonucleotides targeting Nogo-A were ligated to the vector pZDonor-enhanced green fluorescent protein. The shRNA sequence for rat Nogo-A is 5'-GAAGCATGTGAAAGT-GAAGTCAAAGTTCACCTTTCACATGCTTCC-3' and that for control shRNA is 5'-TAATTGTCAAATCAGAGTGCTTCGA-AAAGCACTCTGATTTGACAATTA-3'. Complexes of shRNA and Lipofectamine 2000 (Thermo Fisher Scientific, Waltham, MA, USA) were slowly injected over 5 min. shRNA (10, 1  $\mu$ g/ $\mu$ l) was diluted in 10  $\mu$ l normal saline and mixed gently. Lipofectamine 2000 (15  $\mu$ l) was mixed with 15  $\mu$ l saline. The shRNA and Lipofectamine 2000 were incubated for 20 min to form an shRNA–Lipofectamine 2000 complex at room temperature. The total volume for injection was 50  $\mu$ l. Four days after the injection of Nogo-A shRNA, 25% CFA was injected into the left hind paw

of the rats. Nociceptive responses were measured 1, 2, 6, 24, and 48 h after administration of CFA.

### Assessment of hypersensitivity

Thermal hyperalgesia was assessed with a procedure adopted from Yang *et al.* (30). In brief, animals were allowed to become accustomed to the environment for 20 min before testing. Paw withdrawal latency in response to radiant heat was recorded. A cutoff time of 30 s was enforced to prevent tissue damage. The paw withdrawal latency was recorded and averaged over 5 trials at 5 min intervals. Paw withdrawal latency was measured in a blinded fashion.

The mechanical pain was examined with the von Frey hair test, as described by Chaplan *et al.* (31). A series of von Frey filaments (Stoelting, Wood Dale, IL, USA) ranging from 1.08 to 21.09 g were used to press the surface of the hind paw. Each filament was applied to the midplantar surface until it bent and was kept in this position for 6–8 s. The lowest force that produced responses, such as lifting and licking, was recorded as the withdrawal threshold. The test was repeated 3 times on each paw at an interval of 10 s, to determine the mean withdrawal threshold. Filaments were started from 4.31, and the mechanical threshold (g) was calculated by the formula provided in Chaplan *et al.*

### Immunofluorescence

Adult male Nogo-A KO SD rats, wild-type (WT) littermates, rats treated with Nogo-A antibody or normal goat IgG, and rats treated with Nogo-A shRNA or control shRNA were anesthetized with 10% chloral hydrate (0.3 g/kg, i.p.) and transcardially perfused with saline, followed by 4% paraformaldehyde in PBS. The DRGs were removed, postfixed in 4% paraformaldehyde for 6 h, treated with 20% sucrose (in PBS) for 24 h and then 30% sucrose (in PBS). DRGs were embedded in Tissue-Tek OCT (Sakura Finetek, Torrance, CA, USA), and cryosections (10  $\mu$ m) were collected and stored at  $-20^{\circ}\text{C}$ . Mounted DRG sections were thawed to room temperature. After thorough washing, sections were incubated with Nogo-A antibody (1:200; goat IgG, s-19, sc-11032; Santa Cruz Biotechnology). The sections were incubated in primary antibodies overnight at  $4^{\circ}\text{C}$ . Some sections were incubated together with NgR (1:200, rabbit IgG, AB15138; MilliporeSigma) or TRPV-1 antibody (1:1000, guinea pig anti-TRPV-1 pAb, AB5566; MilliporeSigma). On the next day, sections were washed with PBS 3 times and then incubated with the corresponding secondary antibodies. Some sections of rats treated with Nogo-A antibody or normal goat IgG were directly incubated with the secondary antibody to identify the access of Nogo-A antibody to DRG neurons. The secondary antibodies for Nogo-A and GFP were FITC-conjugated donkey anti-goat IgG (1:200; Jackson ImmunoResearch, West Grove PA, USA), for green images, or tetramethylrhodamine (TRITC)-conjugated donkey anti-goat IgG (1:200; Jackson ImmunoResearch), for red images. The corresponding secondary antibodies for NgR and TRPV-1 were TRITC-conjugated donkey anti-rabbit IgG (1:200; Jackson ImmunoResearch) and TRITC-conjugated Alexa Fluor 633-conjugated goat anti-guinea pig IgG (1:200, Thermo Fisher Scientific), respectively. After incubation for 3 h at room temperature, the sections were observed by fluorescence microscopy (BH-2; Olympus, Tokyo, Japan) or confocal microscopy (Olympus). Sections of DRGs treated with Nogo-A shRNA and control shRNA were observed directly.

### Western blot analysis

The naive control and some rats at 0.5, 1, 2, 6, and 24 h after injection with 25% CFA in the left paw were deeply anesthetized with 10% chloral hydrate (0.3 g/kg, i.p.) The rats pretreated with NEP 1-40

peptide (30  $\mu$ g), Nogo-A antibody (0.6  $\mu$ g), Latrunculin (Lat) A (100 ng), calpeptin (10  $\mu$ l, 20 mM), or MDL28170 (25  $\mu$ g) were sacrificed 2 h after CFA injection. The Nogo-A KO rats were euthanized at 72 h after CFA administration. DRGs at L4–L6 of the spinal cord were removed and immediately homogenized in ice-cold lysis buffer. The homogenates were centrifuged at 12,000 g for 5 min at  $4^{\circ}\text{C}$ , and the supernatant was analyzed. Protein concentration was measured with a bicinchoninic acid assay kit (Thermo Fisher Scientific). Each sample (50  $\mu$ g) was boiled for 3–5 min with SDS-PAGE sample buffer, subjected to SDS-PAGE on 10% or 12% running gels, and transferred onto nitrocellulose membranes. The membranes were blocked with 5% nonfat milk in Tris-buffered saline-Tween for 1 h at room temperature and then incubated overnight at  $4^{\circ}\text{C}$  with primary antibody. The blots were then washed 3 times in Tris-buffered saline-Tween. The membranes were incubated with horseradish-conjugated secondary antibody (1:2000, goat anti-rabbit, rabbit anti-goat, or goat anti-mouse; Bio-Rad, Hercules, CA, USA) for 1 h at room temperature. Finally, the blots were developed with a chemiluminescence kit (sc-2048; Santa Cruz Biotechnology).

The following commercially available antibodies were used as primary antibodies: Nogo-A (s-19; 1:100, sc-11032; Santa Cruz Biotechnology), Nogo (N18; 1:200, sc-11027; Santa Cruz Biotechnology), NgR (1:100, AB15138; Millipore), S1PR2 (1:1000, sc-365589; Santa Cruz Biotechnology), TRPV-1 (1:100, sc-12498; Santa Cruz Biotechnology), LIMK1 (1:100, sc-5576; Santa Cruz Biotechnology), p-LIMK (1:500, ab131341; Abcam, Cambridge, United Kingdom), cofilin (1:100, sc-33,779; Santa Cruz Biotechnology), p-cofilin (Ser 3; 1:2000, sc-12912-R/sc-21867-R; Santa Cruz Biotechnology),  $\beta$ -actin (1:2000, TA-09; Zhongshan Golden Bridge Biotechnology, Guangdong, China), and GFP (1: 500, sc-8334; Santa Cruz Biotechnology).

### Lat A treatment

Lat A (MilliporeSigma) was dissolved in DMSO (2  $\mu$ g/ $\mu$ l stock solution) and diluted in saline to a final concentration of 10 ng/ $\mu$ l. The same concentration of DMSO in saline was used as a control (vehicle). Five days after placement of the intrathecal catheter, the basal level of paw withdrawal latency was measured. Rats were then subjected to intrathecal injection of Lat A at a dose of 100 ng. A half hour later, 25% CFA was injected into the plantar surface of the left hind paw. The rats were euthanized after injection of 10% chloral hydrate (0.3 g/kg, i.p.). Tissues were collected or DRG neurons were isolated at 2 h after CFA injection.

### F-actin/G-actin *in vivo* assay

The actin polymerization assay in DRGs was analyzed with a Filamentous (F)-Actin/Globular (G)-Actin *In Vivo* Assay Kit (BK037; Cytoskeleton, Denver, CO, USA), and the ratio of F-actin:G-actin was measured. In brief, the rats were deeply anesthetized with 10% chloral hydrate (0.3 g/kg, i.p.). The DRGs at L4–L6 were collected and homogenized in F-actin stabilization buffer. The tissue lysates were centrifuged at 100,000 g,  $37^{\circ}\text{C}$  for 1 h; the resulting pellet contained F-actin and the supernatant contained G-actin. The supernatant was removed and immediately placed on ice, and 100  $\mu$ l F-actin depolymerization buffer was added to each pellet. The samples were then incubated on ice for 1 h. Equal volumes of G- and F-actin samples were mixed with SDS sample buffer, run on 12% SDS polyacrylamide gels, and subjected to immunoblot analysis.

### Isolation of DRG neurons and $\text{Ca}^{2+}$ imaging

Isolation of DRG neurons and  $\text{Ca}^{2+}$  imaging experiments were performed as described by Xing *et al.* (32). Heterozygous (Het) rats or rats injected intrathecally with the following were used: 1) 30  $\mu$ l NEP 1-40 peptide (1  $\mu$ g/ $\mu$ l) or scrambled peptide (1  $\mu$ g/ $\mu$ l); 2) 3  $\mu$ l

Nogo-A antibody (0.2  $\mu\text{g}/\mu\text{l}$ ) or normal goat IgG; and 3) 100 ng Lat A or vehicle. CFA (100  $\mu\text{l}$  of 25% solution) was injected into the left hind paw 0.5 h after the intrathecal injection. Rats were terminated with an overdose of anesthetic 1–2 h after CFA injection. The left L4–L5 DRGs were removed and digested with collagenase type IA (1.5 mg/ml; MilliporeSigma) for 50 min and then with 0.125% trypsin (MilliporeSigma) for 8–10 min at 37°C. The enzymatic treatment was terminated by fetal bovine serum. The DRGs was dissociated by gentle trituration with a flame-polished Pasteur pipette and centrifuged at 500 rpm for 3 min. The cell pellet was resuspended in DMEM. The dissociated cells were plated on poly-D-lysine-coated (100  $\mu\text{g}/\text{ml}$ ; MilliporeSigma) glass coverslips inside 35- $\mu\text{m}$  culture dishes with a 10- $\mu\text{m}$ -diameter well and kept for 1.5 h at 37°C.

The DRG cells were washed with Dulbecco's PBS (NaCl 0.8%,  $\text{Na}_2\text{HPO}_4$  0.29%, KCl 0.02%,  $\text{KH}_2\text{PO}_4$  0.02%,  $\text{MgCl}_2$  0.01%, and  $\text{CaCl}_2$  0.01%; pH adjusted to 7.4–7.6) containing 1% bovine serum albumin and incubated in Fura-2 AM (5  $\mu\text{M}$ ; Thermo Fisher Scientific) in DPBS at room temperature for 30 min. The cells were washed with Dulbecco's PBS and incubated in Neurobasal medium without phenolsulfonylphthalate in room temperature in the dark for a 1 h recovery. For calcium imaging, an inverted fluorescence microscope equipped with 340 and 380 nm excitation filter sets (Olympus) and a computer with Metafluor software (Molecular Devices, Sunnyvale, CA, USA) was used. Fluorescence images and the F340:F380 ratio were acquired every 10 s. TRPV-1 activation was evoked by the addition of capsaicin. After acquisition of 10 images for baseline, capsaicin was added with a final concentration of 5  $\mu\text{M}$ , and a rapid, robust increase in intracellular  $\text{Ca}^{2+}$  was acquired.

## Statistical analysis

All data are presented as means  $\pm$  SEM. Statistical analyses were performed with Prism 6.0 software (GraphPad, La Jolla, CA, USA). Differences between experimental and control groups were compared by using either Student's *t* test or 1-way ANOVA followed by Newman-Keuls *post hoc* test or 2-way ANOVA followed by Bonferroni's *post hoc* test. Statistical significance was set at  $P < 0.05$ .

For Western blot analysis, films were scanned with ImageJ software (National Institutes Health, Bethesda, MD, USA), and the densities of relevant bands were measured. All the protein expression levels were normalized with their own internal loading controls. The experimental groups were normalized with the control groups. The data were analyzed by Prism 6.0, using the tests previously described.

## RESULTS

### Nogo-A was upregulated in DRG neurons after CFA injection

Immunohistochemistry showed a localization of Nogo-A protein in some DRG neurons in wide-type (WT) adult rats and was undetectable in the DRGs from Nogo-A KO rats (Fig. 1A). Nogo-A was found in neurons of different sizes, but was particularly prominent in the small- and medium-sized cells. Pain was generated by an injection of CFA into the left hind paw. The CFA injection produced an obvious increase in Nogo-A protein in DRGs collected from L4–L6 vertebrae throughout the period of observation (0.5–24 h) (Fig. 1B). Quantitative analysis of the Western blot results demonstrated a significant elevation of Nogo-A protein

shortly after CFA injection, with a 1-fold increase 0.5 h after pain induction, and that level was maintained up to 24 h (Fig. 1B).

To determine whether NgR is localized in Nogo-A-expressing neurons, sections of naive DRGs contralateral to the injected hind paw were immunostained simultaneously with Nogo-A and NgR antibodies. NgR was colocalized on most Nogo-A-positive neurons in the DRGs (Fig. 1C), which was consistent with previous findings showing localization of NgR on the surface of adult rat DRG neurons (33, 34). The changes in NgR level at different time points (1–24 h) after CFA injection were assessed by Western blot, which showed a stable expression throughout the period of the experiment (Fig. 1D).

### Disruption of NgR activity by Nogo-66 antagonist peptide reduced CFA-induced inflammatory heat hyperalgesia

To investigate whether the elevated levels of Nogo-A contribute to the induction of pain hypersensitivity, 2 antagonists of Nogo-A signaling were intrathecally infused 30 min before injection of CFA. These antagonists included 1) NEP 1-40, corresponding to the N-terminal residues 1–40 of Nogo-66, which has been shown to inhibit axonal outgrowth through binding to the Nogo-66 receptor (NgR) (29); and 2) JTE-013 (the antagonist for the receptor of Nogo-A  $\Delta 20$ -S1PR2) (25).

Paw withdrawal latency in response to radiant heat in both groups was measured during the 24-h period after CFA injection in accordance with a protocol published by Ji *et al.* (35). Although NEP 1-40 produced no detectable effect at low dose (3  $\mu\text{g}$ ) when compared with the control injected with scrambled peptide (Fig. 1E), it significantly increased the withdrawal latency in the ipsilateral paw at higher doses (10 and 30  $\mu\text{g}$ ) (Fig. 1F, G). The differences were most obvious at 2 h after CFA injection, when the amount of Nogo-A protein peaked. However, injection of NEP 1-40 at these high doses did not produce any detectable change in paw withdrawal latency in the contralateral noninjected paw (Supplemental Fig. 1A, B). The mechanical pain of the ipsilateral paw was also measured by the von Frey hair test (31). The results showed that NEP 1-40 did not produce a significant change in the mechanical pain at the doses that attenuate heat hyperalgesia (Supplemental Fig. 1C, D). Nevertheless, intrathecal injection of JTE-013 at 0.1, 1.0, and 10  $\mu\text{g}$  consistently did not affect the ipsilateral paw withdrawal latency in the CFA-injected paw (Supplemental Fig. 1E), suggesting that the Nogo- $\Delta 20$  fragment may not be involved in inflammatory heat hyperalgesia. Furthermore, the expression of S1PR2 was analyzed by Western blot in DRGs and cerebral cortex. It was found that S1PR2 was not detected on the adult DRGs, with or without CFA, although it was obviously expressed in the cerebral cortex at the predicted molecular mass of 39 kDa (Supplemental Fig. 1F). These findings suggest that Nogo-A/NgR signaling is involved in the induction of inflammatory heat hyperalgesia and that this interaction is probably mediated by the Nogo-66 domain, but not by Nogo- $\Delta 20$ .

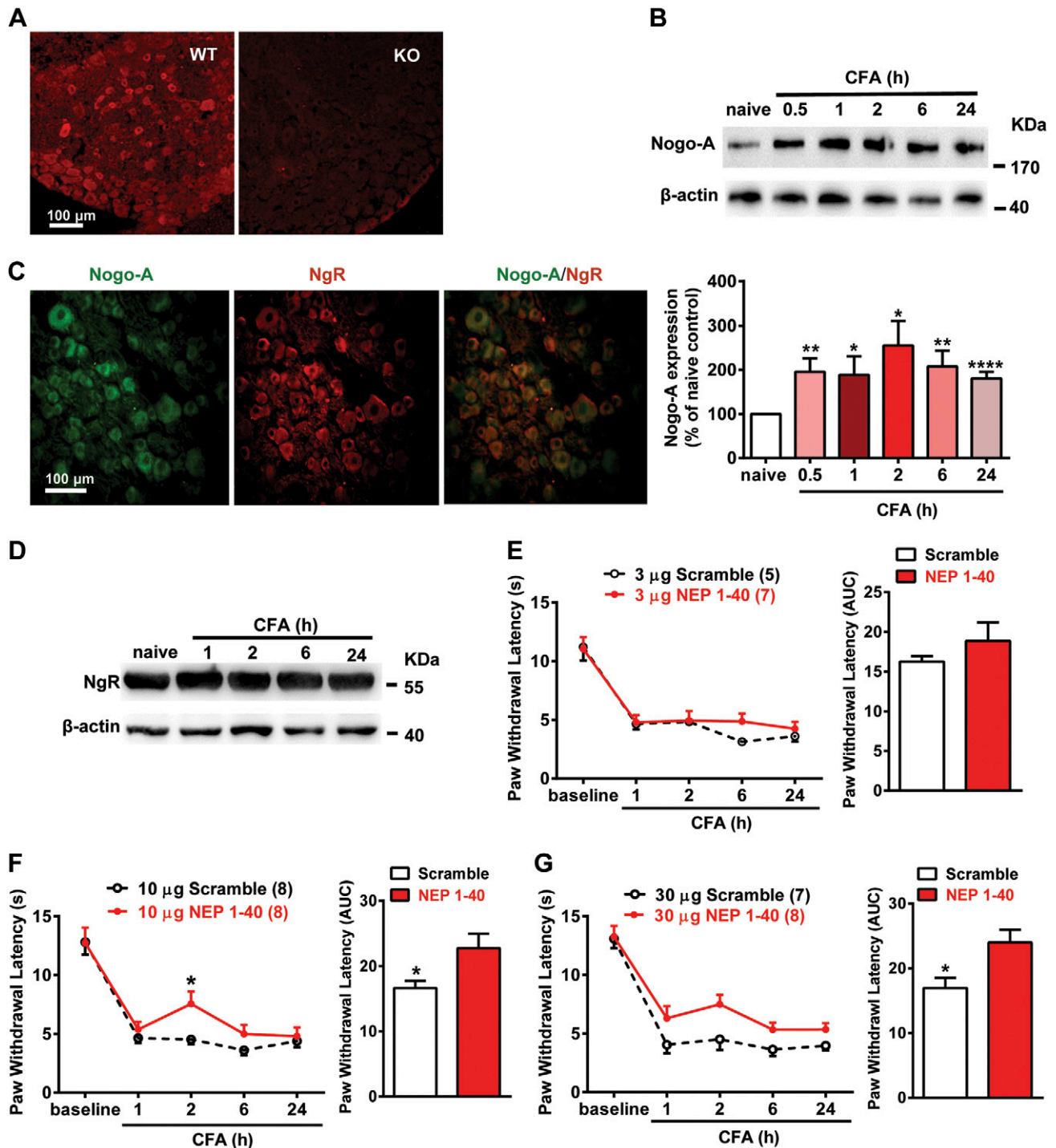


**Figure 1.** The elevation of Nogo-A in adult rat DRGs is involved in heat hyperalgesia. **A)** Immunofluorescence showed that Nogo-A (red) protein was expressed intensely in the DRG neurons of WT rats, but not in sections of Nogo-A<sup>-/-</sup> (KO) rats. **B)** Western blot analysis showed that the amount of Nogo-A in DRGs increased significantly from 0.5 to 24 h after CFA injection. Values are means  $\pm$  SEM (3 independent experiments). \* $P$  < 0.05, \*\* $P$  < 0.01, \*\*\*\* $P$  < 0.0001 vs. naive control (ANOVA, followed by Dunnett's multiple-comparison test). **C)** Nogo-A protein (green) was colocalized with NgR (red) in DRG neurons of naive adult rats. The double-labeled neurons appeared yellow. **D)** Western blot analysis showed that the expression of NgR in DRGs did not change obviously after CFA injection (3 independent experiments). **E–G)** Intrathecal injection of NEP 1-40 peptides (the antagonist peptide for NgR) attenuated the heat hyperalgesia in CFA-induced inflammatory pain. Left: time courses of paw withdrawal latency after intrathecal injection of 3 (**E**), 10 (**F**), and 30  $\mu$ g (**G**) NEP 1-40 or scrambled peptide. Data are means  $\pm$  SEM; 2-way ANOVA, followed by the Bonferroni *post hoc* test, compared with the same amount of control peptide at corresponding time points. \* $P$  < 0.05 compared with the scrambled peptide groups. Right: quantification analysis of the areas under the curve (1–24 h) after intrathecal injection of antagonist peptides NEP 1-40 or the control peptide. Data were analyzed by unpaired Student's *t* test ( $n$  = 5–8). \* $P$  < 0.05 vs. the scrambled peptide groups. Scale bars, 100  $\mu$ m.

## Nogo-A antibody, Nogo-A shRNA, and genetic deletion of Nogo-A attenuated CFA-induced heat hyperalgesia

The specificity of Nogo-A in CFA-induced heat hypersensitivity was determined with a Nogo-A-specific antibody and Nogo-A shRNA, and in rats with Nogo-A KO. Nogo-A antibody was injected intrathecally to block the function of Nogo-A in DRGs. This antibody recognizes the epitope within the Nogo-A-specific domain that is not shared with other known Nogo isoforms. Nogo-66 and Nogo- $\Delta$ 20 fragment are not recognized by this antibody.

The specificity of this antibody was confirmed by Western blot analysis of the DRG tissues, with or without CFA administration (Supplemental Fig. 2A). This antibody revealed a major band of Nogo-A at  $\sim$ 200 kDa and it increased obviously at 2 h after CFA injection. Although infusion of Nogo-A antibody at a low dose (0.2  $\mu$ g; Supplemental Fig. 2B) did not produce an obvious change in the withdrawal latency of the ipsilateral paw, antibody at higher doses (0.6 or 2.0  $\mu$ g) significantly increased the withdrawal latency when compared with treatment with normal goat IgG (Fig. 2A, B). This result indicates that another functional domain of Nogo-A (not Nogo- $\Delta$ 20) in

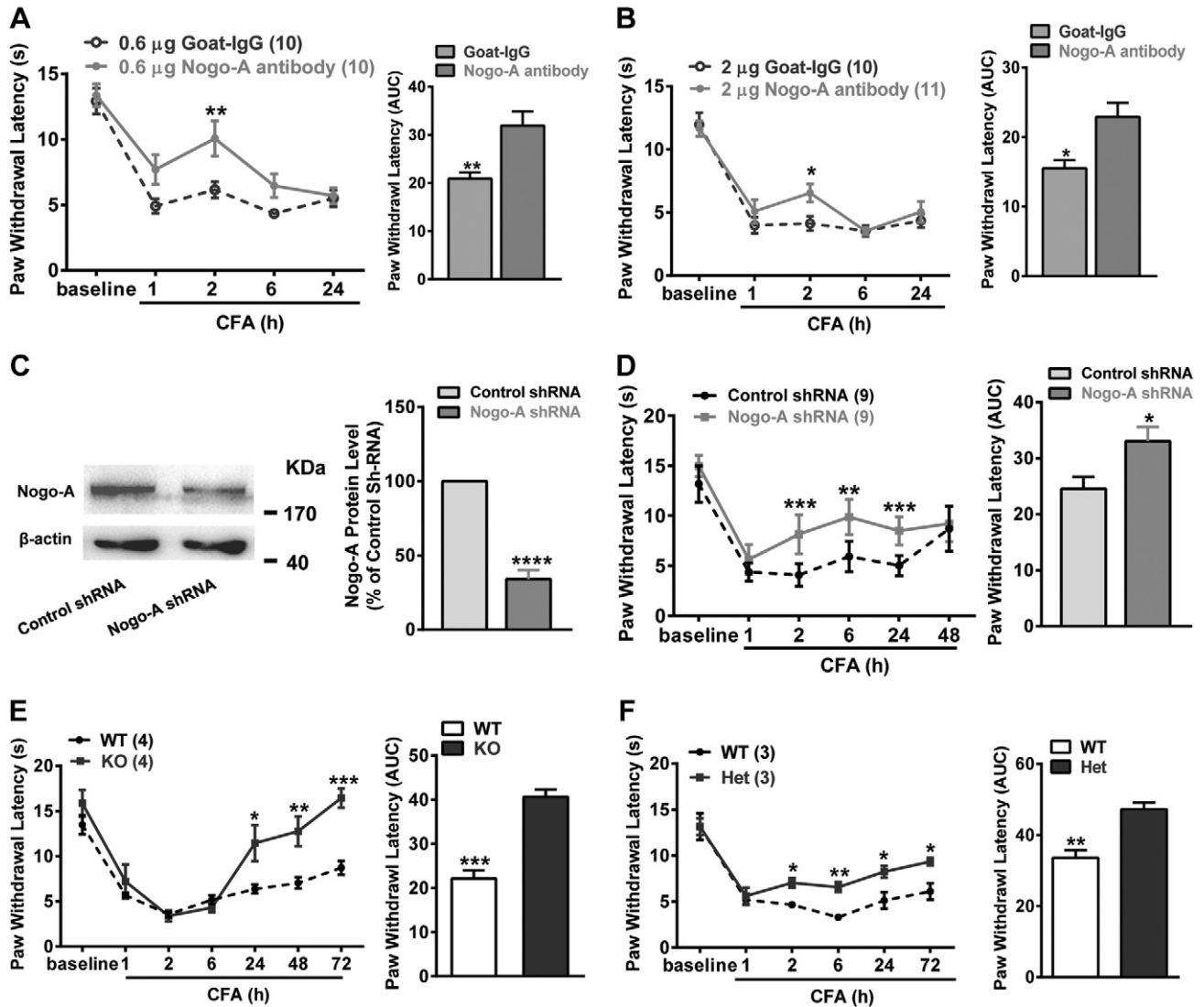


**Figure 2.** Intrathecal injection of Nogo-A-specific antibody, Nogo-A shRNA, or genetic deletion of Nogo-A protein consistently showed that disruption of Nogo-A function attenuates the heat hyperalgesia in CFA-induced inflammatory pain. *A, B*) Intrathecal injection of a Nogo-A antibody at high dosage attenuated the inflammatory heat hyperalgesia (3 independent experiments). \* $P < 0.05$ , \*\* $P < 0.01$ . *C*) The expression of Nogo-A was efficiently knocked down by the intrathecal injection of Nogo-A shRNA 2 h after CFA injection (9 independent experiments). \*\*\*\* $P < 0.0001$  compared with the control shRNA (by ANOVA followed by Dunnett's multiple-comparison test). *D*) Time course of paw withdrawal latency and quantification analysis of the area under the curve (1–48 h) showed that knockdown of Nogo-A by intrathecally injected Nogo-A shRNA significantly attenuated inflammatory heat sensitivity. \* $P < 0.05$ , \*\* $P < 0.01$ , \*\*\* $P < 0.001$  vs. control. *E, F*) Time course of paw withdrawal latency (left) and quantification analysis of the area under the curve (right) in KO (*E*) and Het rats (*F*) after CFA injection compared with WT. *A, B, D–F*) Data are means  $\pm$  SEM. In the left plots, data were analyzed by 2-way ANOVA, followed by the Bonferroni *post hoc* test, compared with control IgG, control shRNA, or WT at the corresponding time points. Right: data were analyzed by unpaired Student's *t* test. \* $P < 0.05$ , \*\* $P < 0.01$ , \*\*\* $P < 0.001$  vs. the control groups.

addition to Nogo-66 also mediated the heat hyperalgesia after CFA injection. Treatment with the Nogo-A antibody did not produce any detectable difference in paw withdrawal latency on the contralateral noninflamed hind paw at both doses, when compared with those injected with goat IgG (Supplemental Fig. 2C, D). Moreover, the mechanical pain in the ipsilateral paw was not obviously changed when treated with the Nogo-A antibody (Supplemental Fig. 2E). To verify the accessibility to injected antibody, Nogo-A antibody was detected in sections of DRGs with an FITC-conjugated donkey anti-goat secondary antibody 2 h after CFA injection, when the analgesic effect was most prominent. The results showed that intense fluorescent signals were observed on DRG neurons pretreated with Nogo-A antibody injection, but no signal was detected in those treated with normal goat IgG, indicating that the antibody infused into the DRGs and bound to Nogo-A on the neurons (Supplemental Fig. 2F).

In another experiment, Nogo-A shRNA plasmid was injected intrathecally to knock down Nogo-A in DRG neurons. Western blot analyses results showed that Nogo-A protein was reduced significantly in DRGs after treatment of Nogo-A shRNA, when compared with that treated with control shRNA (Fig. 2C). Nogo-A shRNA (10  $\mu$ g) significantly increased the ipsilateral paw withdrawal latency at 2, 6, and 24 h after CFA injection, when compared with that treated with the control shRNA (Fig. 2D). Analysis of the area under the curve indicated that knockdown of Nogo-A attenuated significantly the CFA-induced heat hyperalgesia (Fig. 2D). The successful transfection of shRNAs was confirmed by immunohistochemistry (Supplemental Fig. 3A) and Western blot (Supplemental Fig. 3B), which showed the expression of GFP in the DRG neurons.

The involvement of Nogo-A in inflammatory heat hyperalgesia was also examined in Nogo-A KO rats. The KO animals were generated with the CRISPR/Cas9 system. The gRNAs were designed targeting the exon 3 of the rat *Rtn4* gene, which is specific to Nogo-A (Supplemental Fig. 4A). In adult KO rats, Nogo-A was undetectable in the spinal cord, cerebral cortex (Supplemental Fig. 4B), and DRGs (Fig. 1A and Supplemental Fig. 4C), whereas it was highly expressed in WT animals. Nogo-A in DRGs of Het animals was reduced almost by half (Supplemental Fig. 4C). The paw withdrawal latency in Nogo-A KO rats was significantly increased 24 h after CFA injection, and this effect lasted up to 72 h, the latest time point examined (Fig. 2E). In Nogo-A Het rats, the ipsilateral paw withdrawal latency was increased significantly 2 h after CFA injection, similar to the effects produced with the NgR antagonist, blocking antibody, and shRNA, and the effect lasted up to 72 h after CFA injection (Fig. 2F). These findings confirm that Nogo-A is necessary to generate the heat hypersensitivity induced by CFA. The local inflammatory response around the injection site was evaluated by measuring the volume of paw swelling. Knockout of Nogo-A did not obviously change the CFA-induced inflammation, as indicated by the volume of swelling (Supplemental Fig. 4D). Moreover, the contralateral paw withdrawal latency in both Het and KO rats was not obviously changed (Supplemental Fig. 4E, F). The mechanical pain in the ipsilateral paw showed no obvious change between the WT and Nogo-A KO rats within 72 h after CFA injection (Supplemental Fig. 4G).

## NEP 1-40 peptide, Nogo-A antibody, and a genetic knockdown all impaired the response of TRPV-1 channel to capsaicin

TRPV-1 is the pivotal nociceptive receptor in DRG neurons that mediates inflammatory thermal nociception. Knockout mice lacking TRPV-1 do not develop heat hyperalgesia after inflammation (1, 2). In our study, we investigated whether Nogo-A may regulate inflammatory heat hyperalgesia through a modulation of TRPV-1 function. First, we examined whether Nogo-A is colocalized with TRPV-1 in DRG neurons. Immunofluorescence staining showed that there were only a few Nogo-A and TRPV-1 double-labeled neurons in the naive DRGs; whereas the number of double-labeled neurons was dramatically increased in DRGs 2 h after CFA administration (Fig. 3A). The increase in Nogo-A/TRPV-1<sup>+</sup> neurons was confirmed by counting the number of double-stained neurons among the small- and medium-sized neurons. These results support the idea that CFA stimulates an increase in TRPV-1 activity *via* Nogo-A in DRG neurons.

Using Fura-2 AM, calcium imaging experiments were performed in acutely dissociated DRG neurons isolated from Het rats or rats with intrathecal injection of antagonist peptide or Nogo-A antibody 2 h after CFA injection. The NgR antagonist peptide NEP 1-40 significantly suppressed the rapid and robust increase in intracellular Ca<sup>2+</sup> triggered by 5  $\mu$ M capsaicin, which is known to bind to TRPV-1, when compared with treatment with control scrambled peptide (Fig. 3B). Similar effects were observed with Nogo-A blocking antibody or genetic knockdown of Nogo-A in Het rats (Fig. 3C, D), when compared with treatment with normal Goat IgG or WT animals. These results indicate that interruption of Nogo-A signaling inhibits the capsaicin-stimulated activity of the TRPV-1 channel during inflammatory pain hypersensitivity.

## Disruption of Nogo-A signaling dramatically reduced the protein amount of TRPV-1 in DRGs of rats with CFA injection

A possible mechanism that reduces the calcium response of DRGs to capsaicin after disruption of Nogo-A signaling is down-regulation of the TRPV-1 channel. Western blot analysis showed that without CFA injection, intrathecal infusion of the NgR antagonist peptide NEP 1-40 did not affect the level of TRPV-1 in the DRGs (Fig. 4A). However, the antagonist peptide caused a significant reduction in the elevated expression of TRPV-1 caused by CFA injection, when compared with scrambled peptide (35, 36) (Fig. 4B). Similarly, Nogo-A antibody treatment or KO of Nogo-A from DRGs at the time when the heat hyperalgesia was significantly attenuated, did not obviously alter the level of TRPV-1 in DRGs in the absence of CFA injection (Fig. 4C, E), but significant down-regulation of the TRPV-1 protein was observed with CFA injection when compared with normal IgG treatment or WT animals (Fig. 4D, F). Hence, we concluded that Nogo-A signaling is necessary to maintain the elevated function of TRPV-1 during inflammatory pain hypersensitivity.

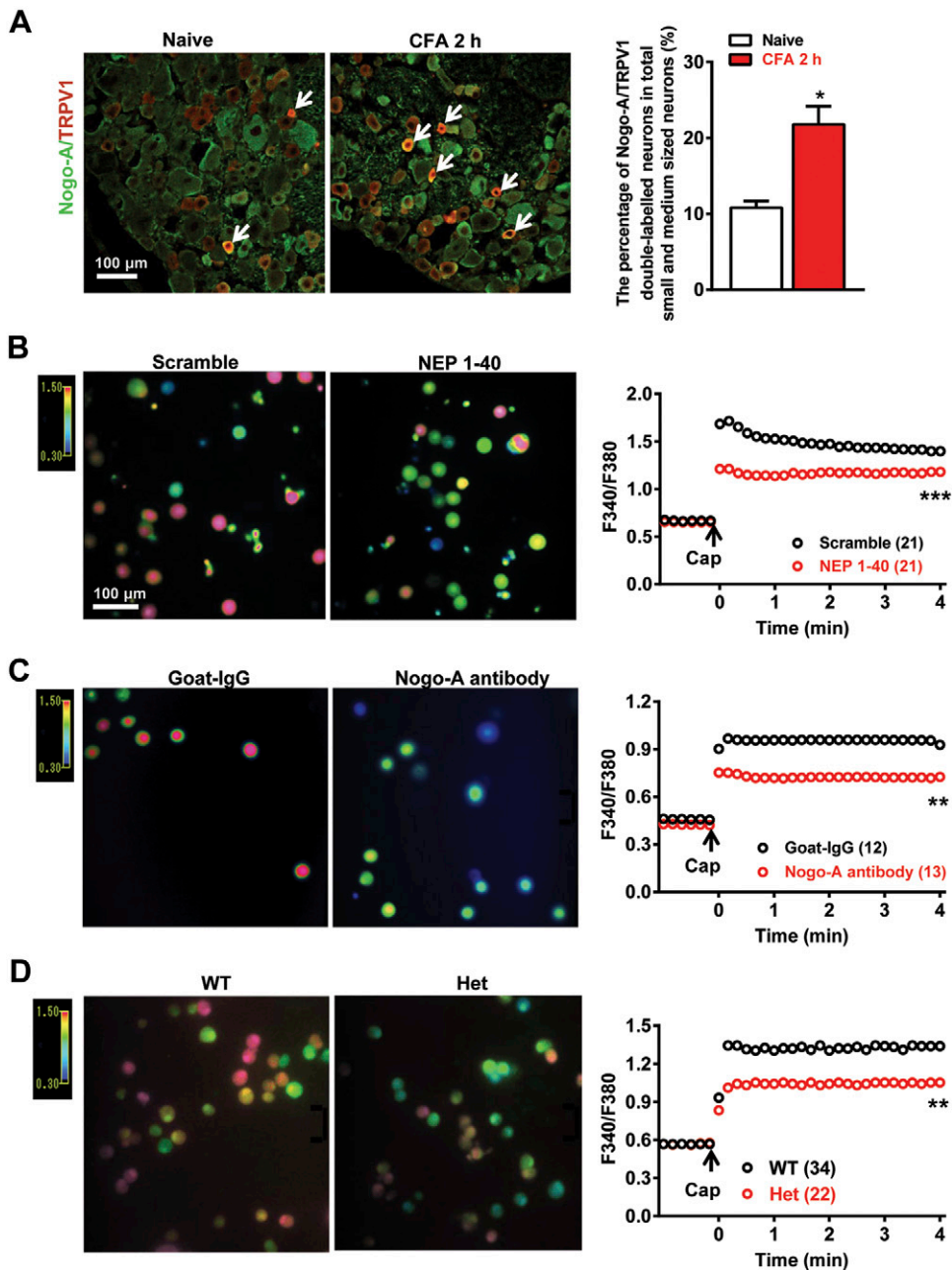


**Figure 3.** Disruption of Nogo-A signaling by intrathecal injection of NPEP 1-40 peptide, Nogo-A antibody, or genetic knock-down impaired the intracellular  $\text{Ca}^{2+}$  signal in response to capsaicin in DRG neurons. **A)** The colocalization (arrows, yellow) of Nogo-A (green) and TRPV-1 (red) was found in DRGs of the naive rats and rats at 2 h after CFA administration. The percentage of double-labeled neurons in the total small and medium-sized neurons increased dramatically after CFA injection compared with that of the naive rat (3 independent experiments).  $*P < 0.05$ . **B-D)** Comparison of intracellular  $\text{Ca}^{2+}$  signal in response to capsaicin in DRG neurons isolated from rats with intrathecal injection of NPEP 1-40 peptide (**B**, left), Nogo-A antibody (**C**, left), or genetic knockdown of Nogo-A (**D**, left) with that of the corresponding controls. The statistical analysis of the F340:F380 ratio showed that intrathecal injection of NPEP 1-40 (**B**, right), Nogo-A antibody (**C**, right), or genetic knockdown of Nogo-A (**D**, right) significantly decreased the response of the TRPV-1 channel to capsaicin, compared with the corresponding control. Data were analyzed by 2-way ANOVA, followed by the Bonferroni *post hoc* test, compared with the corresponding control group (3 independent experiments).  $**P < 0.01$ ,  $***P < 0.001$  vs. the corresponding control groups.

### Nogo-A triggered the activation of the LIMK/cofilin pathway and polymerization of actin in CFA-induced inflammatory pain hypersensitivity

Nogo-A may modulate TRPV-1 function through its downstream intracellular signaling pathways. Because LIMK and the actin regulator cofilin have been reported to mediate the Nogo-A function (19, 24), we hypothesized that the LIMK/cofilin/actin pathway is likely to be the downstream pathway that mediates the function of Nogo-A in inflammatory pain. To investigate this possibility, we examined the changes in phosphorylated LIMK, phosphorylated cofilin, and the ratio of polymeric F-actin to monomeric G-actin (indicating the actin filament polymerization) in DRGs of rats after CFA injection. The results

showed that phosphorylated LIMK (Fig. 5A, D) and phosphorylated cofilin (Fig. 5B, E) were reduced significantly 2 h after CFA injection in DRGs of rats treated with NPEP 1-40 peptide or Nogo-A antibody. The total LIMK and total cofilin levels were not affected in both groups. Similar results were obtained from DRGs of Nogo-A KO rats 72 h after CFA injection, where the phosphorylated forms of LIMK and cofilin were reduced significantly, when compared with the levels in WT (Fig. 5G, H). Moreover, Nogo-A antibody, NPEP 1-40, or Nogo-A KO decreased the ratio of F-actin:G-actin significantly in the DRGs ipsilateral to CFA injection, when compared with the corresponding controls (Fig. 5C, F, I), indicating a clearly negative effect of blocking Nogo-A signaling on actin filament assembly in CFA-induced inflammatory pain. In summary, these findings support that Nogo-A



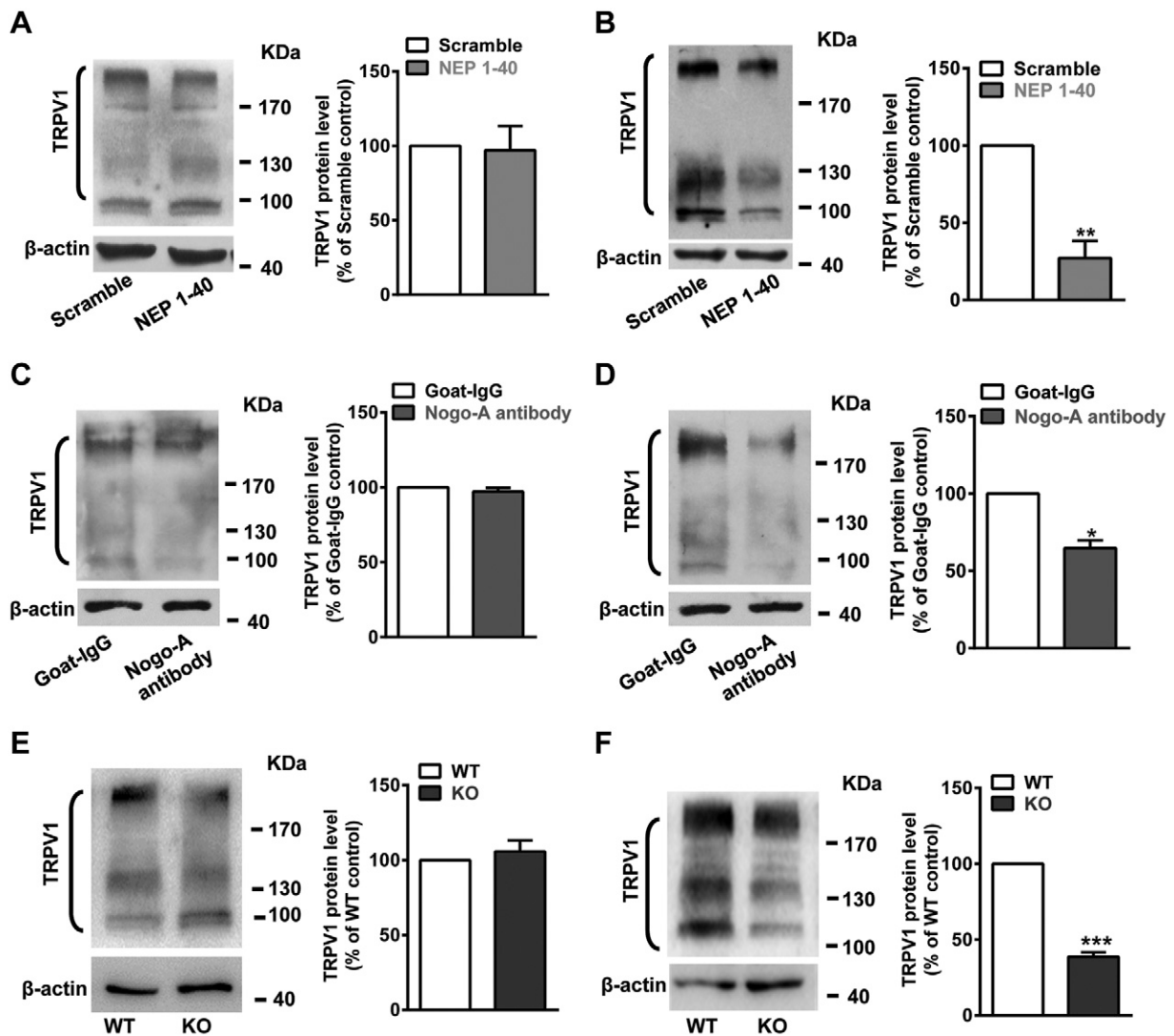


**Figure 4.** Disruption of Nogo-A signaling with NEP 1-40 peptide, Nogo-A antibody, or genetic deletion dramatically decreased the amount of TRPV-1 in the DRGs of rats after CFA injection. *A, C, E* Western blot and quantitative analyses of TRPV-1 in contralateral DRGs without CFA injection demonstrated that intrathecal infusion of NEP 1-40 (*A*), Nogo-A antibody (*C*), or genetic deletion (*E*) did not affect the basal expression of TRPV-1 in rats. In our experiment, the bands of the monomer, glycosylation, and polymerization of TRPV-1 were included for quantification of the amount of TRPV-1. *B, D, F* Western blot and quantitative analyses of TRPV-1 demonstrated disruption of Nogo-A signaling with intrathecal infusion of NEP 1-40 (*B*), Nogo-A antibody (*D*), or genetic deletion (*F*) significantly decreasing the amount of TRPV-1 in DRGs of rats with CFA injection. Data are means  $\pm$  SEM ( $n = 3-7$ ). \* $P < 0.05$ , \*\* $P < 0.01$ , \*\*\* $P < 0.001$  vs. the corresponding control group (unpaired Student's *t* test).

signals through the LIMK/cofilin pathway to stimulate polymerization of actin filaments in CFA-induced inflammatory pain hypersensitivity.

### Disruption of actin microfilament with Lat A decreased the protein amount and function of TRPV-1

To determine whether the disassembly of actin microfilament architecture causes the down-regulation of TRPV-1, the intracellular calcium level was investigated in DRG neurons after treatment with an intrathecal infusion of the microfilament disruptor Lat A. The imaging results showed that Lat A significantly reduced the increase of intracellular  $Ca^{2+}$  triggered by capsaicin when compared with vehicle (Fig. 6A). Moreover, the elevated level of TRPV-1 protein

triggered by CFA was decreased after Lat A treatment (Fig. 6B), indicating that a breakdown of actin filament architecture, an effect also caused by interrupting Nogo-A functions, results in reduced protein level and function of TRPV-1 in DRG neurons.

### Nogo-A signaling regulated calpain-mediated degradation of TRPV-1

The reduction in TRPV-1 after interruption of Nogo-A signaling could be caused by a promotion of degradation of TRPV-1 protein. To test this hypothesis, NEP 1-40 or scrambled peptide was injected intrathecally 0.5 h after CFA injection, when the TRPV-1 protein level had already started to increase (26). Paw withdrawal latency tests revealed that NEP 1-40 could still attenuate CFA-induced

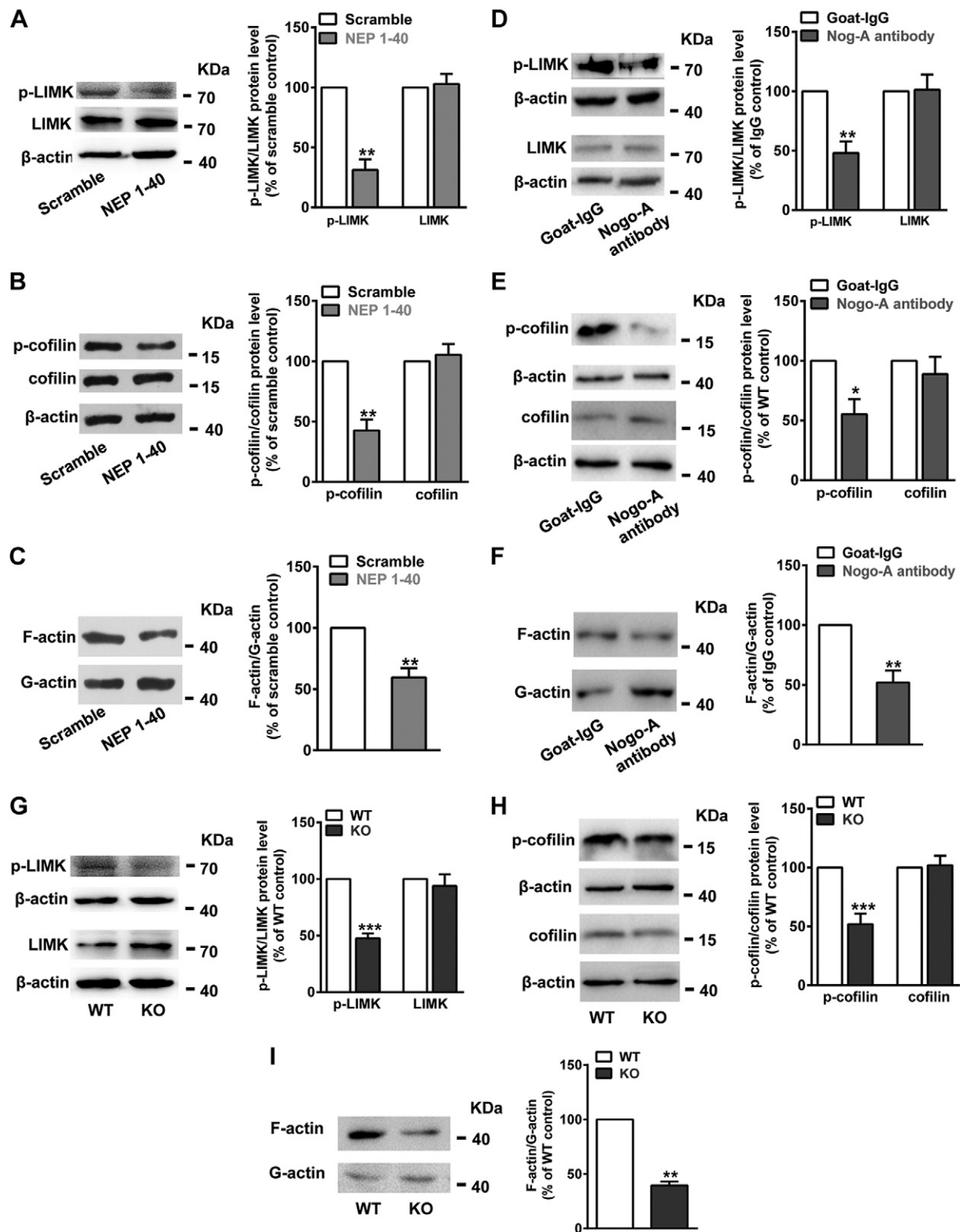


**Figure 5.** Disruption of Nogo-A signaling suppressed phosphorylation of the LIMK and cofilin, resulting in the disassembly of actin microfilament in DRGs of rats after a CFA injection. *A, D, G*) Western blot analysis of phosphorylation of LIMK after intrathecal injection with NEP 1-40, Nogo-A antibody, or Nogo-A KO. Statistical analysis showed that NEP 1-40 (*A*), Nogo-A antibody (*D*), and Nogo-A KO (*G*) significantly decreased the phosphorylation level of LIMK, but had no obvious effect on total LIMK.  $**P < 0.01$ ,  $***P < 0.001$ . *B, E, H*). Western blot analysis showed that NEP 1-40 peptide (*B*), Nogo-A antibody (*E*), and Nogo-A KO (*H*) significantly reduced the phosphorylation level of cofilin.  $*P < 0.05$ ,  $**P < 0.01$ ,  $***P < 0.001$ , but had no influence on total cofilin. *C, F, I*) Western blot and quantification analyses of G- and F-actin levels in DRGs after intrathecal injection of NEP 1-40 peptide (*C*), Nogo-A antibody (*F*), or genetic deletion of Nogo-A (*I*) showed that disruption of Nogo-A decreased the actin filament polymerization induced by CFA administration. Data are means  $\pm$  SEM. Data were analyzed by unpaired Student's *t* test ( $n = 4-7$ ).  $*P < 0.05$ ,  $**P < 0.01$ ,  $***P < 0.001$  vs. corresponding control groups.

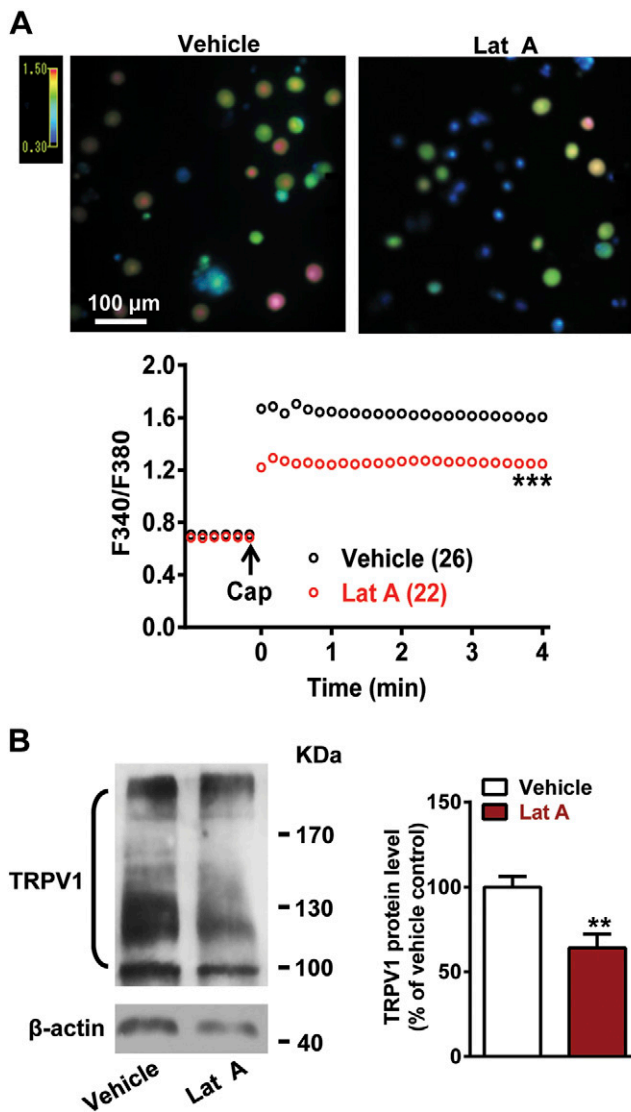


**Figure 6.** Disruption of actin filament directly with Lat A decreased the amount and function of TRPV1 in DRGs of rats after CFA administration. **A)** Comparison of intracellular  $\text{Ca}^{2+}$  signal changes in response to capsaicin of DRG neurons isolated from rats intrathecally treated with 100 ng Lat A or vehicle 2 h after CFA injection. The statistical analysis of the F340:F380 ratio showed that intrathecal injection of Lat A significantly decreased the response of the TRPV-1 channel to capsaicin compared with the corresponding control. Two-way ANOVA, followed by the Bonferroni *post hoc* test.  $***P < 0.001$ , compared with the vehicle group (3 independent experiments). **B)** Western blot and quantitative analyses of TRPV-1 in DRGs after intrathecal injection of 100 ng Lat A or vehicle 2 h after CFA injection. Data are means  $\pm$  SEM (7 independent experiments).  $**P < 0.01$  *vs.* the vehicle group (unpaired Student's *t* test).

heat hypersensitivity (Fig. 7A), and this effect was accompanied by a reduction of the elevated expression of TRPV-1 after CFA treatment (Fig. 7B), likely through degradation of the protein. This degradation process could be mediated by calpain, a family of calcium-dependent neutral proteases, which plays important roles in proteolytic modification of cytoskeletal proteins, receptors, and kinases. Spectrin is an important membrane cytoskeletal protein and serves as a

major substrate for this protease family. The presence of breakdown products of spectrin (135 and 145 kDa) is an indicator of calpain activity (37, 38). In the current study, the spectrin breakdown products were significantly increased in DRGs during inflammation after treatment with NEP 1-40, when compared to treatment with scrambled peptide (Fig. 7C), suggesting that blocking Nogo-A signaling increases calpain activity. Moreover, the calpain-specific inhibitors MDL28170 and calpeptin abolished the effect of NEP 1-40 on the TRPV-1 protein level in DRGs after induction of inflammatory pain by CFA (Fig. 7D, E). These results indicate that disruption of Nogo-A signaling promotes TRPV-1 degradation in a calpain-dependent mechanism.

## DISCUSSION

The major finding in this study is that Nogo-A promotes inflammatory hyperalgesia *via* maintaining TRPV-1 function in DRG neurons. The underlying mechanisms are polymerization of actin *via* LIMK/cofilin pathway and inhibition of calpain-mediated degradation. This modulation of TRPV-1 by Nogo-A signaling underlies a mechanism of CFA-induced inflammatory pain in the adult rat and indicates a major function of Nogo-A in sensory perception in the adult nervous system. Moreover, our results indicated that Nogo-66 functional domain and an undefined amino acid sequence at the N terminus (targeted by Nogo-A antibody) of Nogo-A, but not of Nogo- $\Delta$ 20, play critical roles in this process. The antagonist peptide NEP 1-40 and Nogo-A antibody could be analgesic drugs to alleviate the inflammatory heat hyperalgesia targeting the TRPV-1 channel.

## Nogo-A is involved in the development of heat hypersensitivity in inflammatory pain

It has already been found that the myelin-associated protein Nogo-A is expressed specifically at high levels in adult primary sensory neurons. However, its role in nociception remains to be determined. In a previous study, the heat sensitivity in Nogo-A-deficient mice was examined by the plantar heater test. The results showed that basic heat sensitivity was not affected (39), which is consistent with our results that the paw withdrawal latency of the paw contralateral to the CFA injection did not change obviously in Het or KO rats (Fig. 4E, F). These behavioral results were supported by Western blot analysis, which showed that the basal level of TRPV-1 expression was not affected in DRGs of KO rats in the absence of CFA injection (Fig. 4E). However, the CFA-induced heat hyperalgesia was consistently alleviated after treatment with NEP 1-40, Nogo-A shRNA, or Nogo-A-specific antibody and in Nogo-A KO rats, indicating the crucial role of Nogo-A signaling in promoting inflammatory heat hyperalgesia. Whether Nogo-A is involved in other types of pain perception, such as neuropathic pain, still has not been fully revealed.

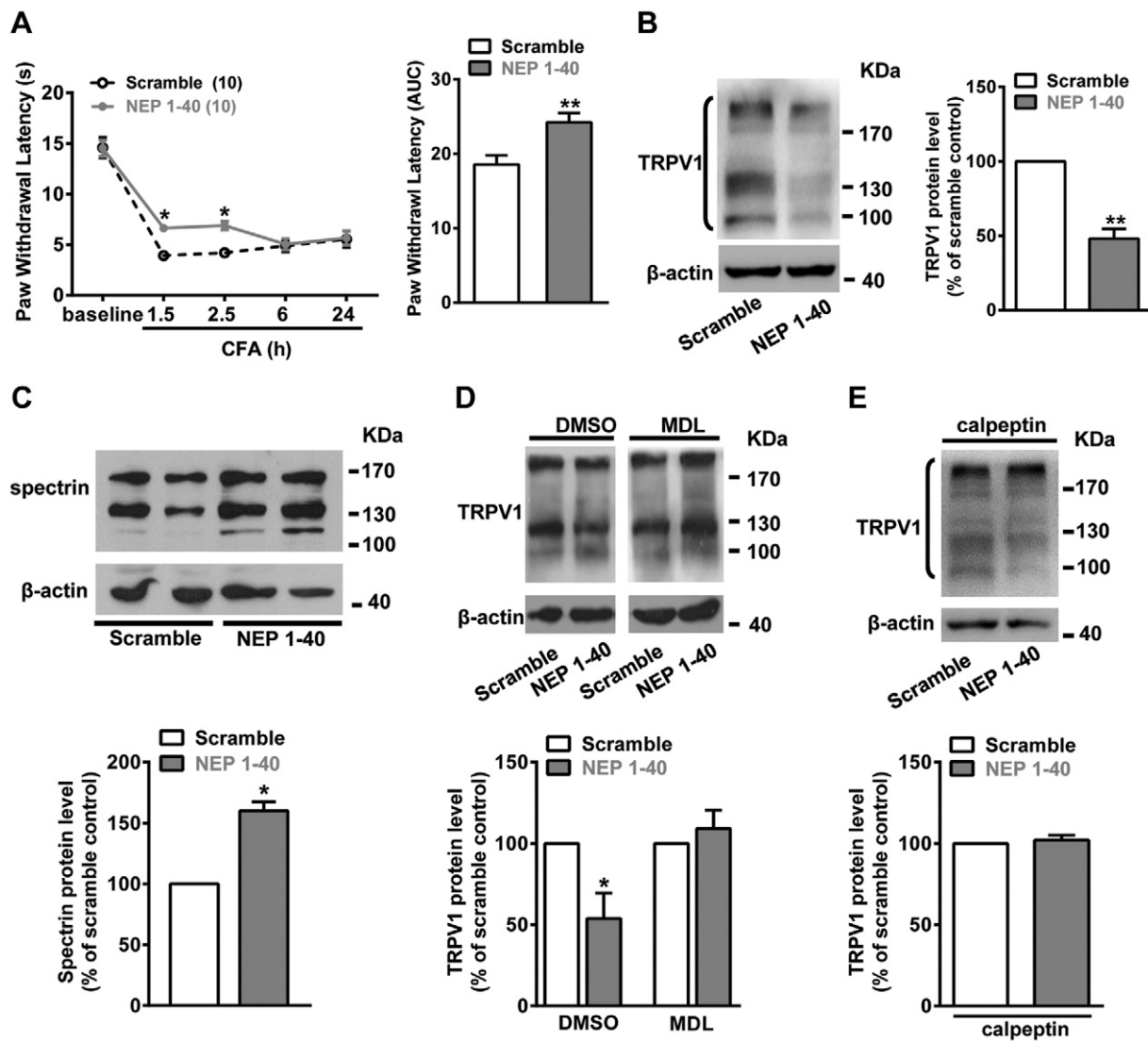


**Figure 7.** Disruption of Nogo-A signaling increases calpain-mediated TRPV-1 degradation in CFA-induced inflammatory heat hyperalgesia. *A, B*) Intrathecal injection of NEP 1-40 at 0.5 h after CFA administration, when the TRPV-1 was already up-regulated, also significantly attenuated the inflammatory heat hyperalgesia and lower the amount of TRPV-1. *A*) Time course of the paw withdrawal latency (left) and quantification analysis of the area under the curve (right) after intrathecal injection of NEP 1-40 or scrambled peptide. *B*) Western blot and quantitative analyses of TRPV-1 in DRGs after intrathecal injection of NEP 1-40 or scrambled peptide 0.5 h after CFA injection. *C*) Western blot and quantitative analyses of spectrin in DRGs of rat 2 h after CFA injection indicated that calpain activity increased significantly after intrathecal injection of NEP 1-40 compared with that of the scrambled peptide. *D*) Western blot and quantitative analyses showed that down-regulation of the TRPV-1 by NEP 1-40 in DRGs after CFA injection was abolished by intrathecal injection of the calpain inhibitor MDL28170. In the DMSO (vehicle) group, NEP 1-40 consistently decreased the TRPV-1 level in DRGs of rats 2 h after CFA injection. However, TRPV-1 did not change obviously after treatment with NEP 1-40 in the group pretreated with MDL28170 (right). *E*) Pretreatment with calpeptin, another calpain activity inhibitor, abolished the down-regulation of NEP 1-40 treatment in the amount of TRPV-1 in DRGs 2 h after CFA injection (shown in Fig. 4*B*). *D* are means  $\pm$  SEM (*A*, left).  $*P < 0.05$  (2-way ANOVA), followed by Bonferroni *post hoc* tests, compared with the scrambled peptide group at corresponding time points; right:  $**P < 0.01$ , unpaired Student's *t* test, *vs.* the scrambled peptide group. Data are means  $\pm$  SEM ( $n = 3-4$  independent experiments) (*B-E*).  $*P < 0.05$ ,  $**P < 0.01$  *vs.* corresponding control group (unpaired Student's *t* test).

### Two functional domains of Nogo-A signal through the LIMK/cofilin/actin pathway in inflammatory hyperalgesia

We also investigated the downstream signaling of Nogo-A that contributes to inflammatory heat hyperalgesia. Our results demonstrated that NEP 1-40 or Nogo-A antibody alleviates CFA-induced heat hyperalgesia, suggesting that both the Nogo-66 domain and the amino acid regions targeted by Nogo-A antibody are major domains involved in the

modulation of hyperalgesia. Nogo- $\Delta 20$ , as another important functional domain of Nogo-A, does not appear to participate in this process. Furthermore, both NEP 1-40 and Nogo-A antibody suppress the activation of LIMK, increase cofilin activity, and destabilize the actin filaments. These phenomena indicate that another amino acid sequence targeted by Nogo-A antibody is likely working through the same downstream pathway as Nogo-66/NgR (19, 24). This amino acid targeted by a Nogo-A-specific antibody should be different from Nogo- $\Delta 20$ , for Nogo- $\Delta 20$  was not involved in the

inflammatory heat hyperalgesia, whereas this Nogo-A antibody attenuated the heat hypersensitivity and change the downstream signaling pathway of Nogo-A. It has been shown that some functional domains at the N terminus of Nogo-A exert synergetic effects with Nogo-66. One example is Nogo-A-24, which is located in an extreme carboxyl region and binds with Nogo-66, forming an NgR ligand with a substantially higher binding affinity than Nogo-66 alone (40). Hence, it is likely that the amino acid sequence targeted by Nogo-A antibody works together with Nogo-66 domain to activate the LIMK/cofilin/actin pathway.

### Nogo-A regulates TRPV-1 function via polymerization of actin filaments in inflammatory heat hyperalgesia

The heat-gated ion channel TRPV-1 is well documented to be a key modulator of inflammatory pain (1, 2). Intact cytoskeleton has been shown to be essential for TRPV-1 to maintain its functions during inflammatory pain. The inflammatory mediators activate cellular kinases, such as p38, PKD, PKA, PKC, and ERK1/2 of the MAPK family, which result in modulating the function of TRPV-1 (35, 36,

41–43). It has been reported that F-actin in DRG neurons constitutes a submembranous network of cytoskeleton, which acts as a scaffold for interactions of pain receptors, downstream kinases, and their effectors (26, 44). Our previous findings have shown that LIMK-dependent actin rearrangement is essential for the development of inflammatory heat hyperalgesia (26). Current results add further that Nogo-A is the upstream molecule of the LIMK/cofilin/actin pathway in this signaling process. This function gains support from the findings that direct reshuffling of actin filaments with Lat A significantly reduces the increase of TRPV-1 in inflammatory DRG neurons and alleviates the response of TRPV-1 to capsaicin. Disturbance of Nogo-A/NgR functions by Nogo-A antibody, NEP 1-40, or genetic Nogo-A KO destabilizes the actin cytoskeleton and produces effects on TRPV-1 functions similar to those induced by Lat A. These findings support strongly that Nogo-A is necessary to maintain the function of TRPV-1, through regulating polymerization of actin filaments in inflammatory heat hyperalgesia. It is worth noting that this Nogo-A-mediated increase in F-actin:G-actin in inflammatory heat hyperalgesia is different from that in neuronal growth cones or hippocampus synapses, where Nogo-A decreases

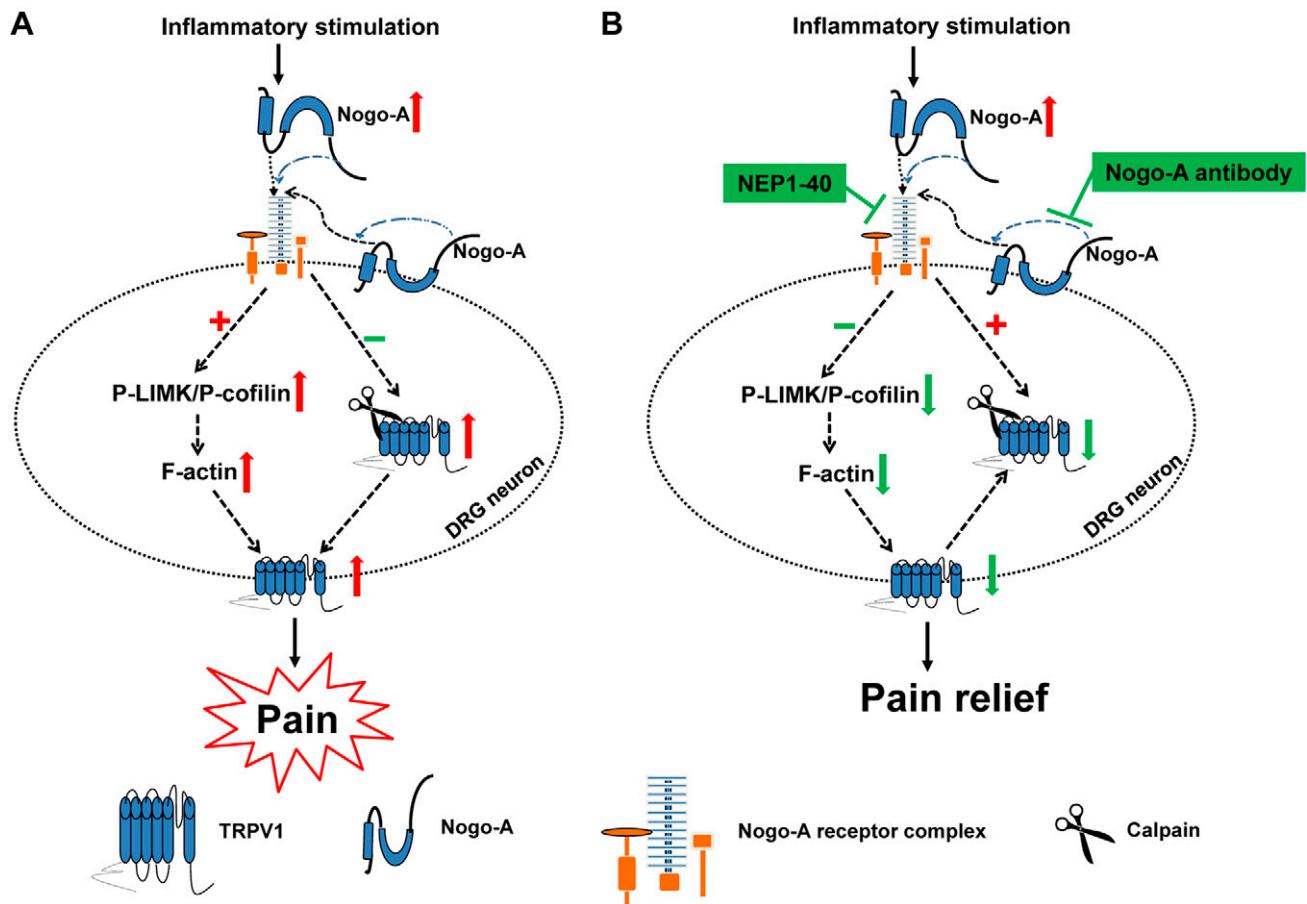


**Figure 8.** Nogo-A signaling in inflammatory heat hyperalgesia. *A*) During inflammation, the Nogo-A protein is up-regulated and binds to its receptor NgR. This interaction of Nogo-A and its receptor increased the phosphorylation level of LIMK and cofilin, which promotes actin polymerization. The polymerized actin filaments may serve as a scaffold for related molecules that support the up-regulation and function of TRPV-1 in inflammatory pain. The up-regulation of TRPV-1 results in an increase in excitability of primary sensory neuron and promotes the development of inflammatory heat hyperalgesia. *B*) When Nogo-A signaling is blocked by NEP 1-40 peptide and Nogo-A antibody, or in KO rat, the phosphorylation of LIMK and cofilin are inhibited and actin filaments depolymerize. Without intact actin cytoskeleton as a scaffold, TRPV-1 is rapidly degraded by proteases such as calpain. Thus pain is relieved.

the phosphorylation of cofilin and the F-actin:G-actin ratio (24, 45, 46). The bidirectional modulation of Nogo-A on actin polymerization suggests that Nogo-A plays distinct roles in actin assembly, depending on the cell type of cells and physiologic processes involved.

The rapid increase in TRPV-1 protein in inflammatory pain is thought to be regulated by posttranslational mechanisms. Inflammation elevates the protein level but not the mRNA level of TRPV-1 in DRG neurons (35, 36, 47). However, the exact mechanism has not been revealed. In this study, NEP 1-40 promoted TRPV-1 degradation with a calpain-dependent mechanism, in addition to its effects on disassembly of actin polymerization. Although it is unclear how Nogo-A affected the degradation of TRPV-1 by calpain in this experiment, the rapid degradation of TRPV-1 by calpain could be a mechanism that underlies the desensitization of TRPV-1.

### Knockout of Nogo-A impairs CFA-induced inflammatory heat hyperalgesia

The essential roles of Nogo-A in inflammatory heat hyperalgesia gains support from the fact that CFA-induced thermal hyperalgesia is significantly attenuated in both Het and KO rats. The absence of Nogo-A is associated with impaired polymerization of actin *via* the LIMK/cofilin pathway during inflammation and with reduction in the protein level of TRPV-1 and its response to capsaicin in DRGs. It is noted that there was a delay in heat hyperalgesia in Nogo-A KO rats, which was only obvious 24 h after CFA injection, when compared with the Het rats, which show effects 2 h after pain induction. The response in Het rats is similar to that treated with Nogo-A shRNA, Nogo-A antibody, or NgR antagonist. The reason for this difference is largely unknown, but is probably not caused by a difference in inflammatory responses induced by CFA between the Het and homogenous mutants, as suggested by measurements of paw volume in these animals. It has been shown in a previous study in mice that the loss of Nogo-A functions in KO mutant can be partly compensated for by the upregulation of other Nogo isoforms, particularly Nogo-B (48). In the present study, the Nogo-B isoform was revealed by the N18 antibody at 53 kDa. It was found that the amount of Nogo-B increased dramatically in the DRGs of KO rats, and its expression level in KO rats did not change obviously within the 72 h after CFA administration (Supplemental Fig. 4H). It is possible that the delayed response observed in the KO rats was due to the increase in production of Nogo-B isoforms, which partly compensated for the loss of Nogo-A during the first 24 h of inflammatory attack. Nevertheless, the findings in these mutants confirm that Nogo-A is essential for generating inflammatory heat hyperalgesia in DRG neurons.

In summary, we have demonstrated a pivotal role of neuronal Nogo-A in DRG neurons in inflammatory heat hyperalgesia (Fig. 8). During inflammatory attacks, Nogo-A protein is up-regulated and stimulates activities of NgR. This interaction increases the phosphorylation of the downstream LIMK and cofilin and results in an increase in actin filament polymerization. The actin filaments serve as a scaffold for maintaining the function of TRPV-1. Nogo-A also enhances TRPV-1 function by inhibiting calpain-mediated TRPV-1

degradation. The increased level of TRPV-1 produces an increase in excitability of primary sensory neurons and promotes the development of inflammatory pain (Fig. 8A). When Nogo-A signaling is blocked by the Nogo-A antibody, the NgR antagonist NEP 1-40, or genetic deletion in KO rats, the phosphorylation of LIMK and cofilin is inhibited, which generates a destabilization of the actin cytoskeleton (Fig. 8B). Without this intact scaffold, TRPV-1 functions are reduced, and the protein may be prone to degradation by proteases such as calpain, resulting in an attenuation of inflammatory pain. FJ

### ACKNOWLEDGMENTS

This work was supported by National Natural Science Foundation of China Grants 31471119 (to J.W.), and 31720103908 and 31530028 (to Y.W.); Beijing Natural Science Foundation Grant 7132130 (to J.W.); Ministry of Science and Technology of China 973 Program Grant 2014CB542204 (to Y.W.); National Science and Technology Support Project Grant 2015BAI08B02 (to Y. W.); and General Research Fund of Hong Kong Research Grant Council Project Grants CUHK461612 and CUHK14113815 (to S.-O.C.). The authors declare no conflicts of interest.

### AUTHOR CONTRIBUTIONS

Y. Wang and J. Wang designed the research and supervised the project; F. Hu, H.-C. Liu, D.-Q. Su, and H.-J. Chen performed the experiments and analyzed the data; H.-C. Liu and J. Wang analyzed the data; F. Hu, S.-O. Chan, and J. Wang wrote the manuscript; and all authors read and approved the manuscript.

### REFERENCES

1. Caterina, M. J., Leffler, A., Malmberg, A. B., Martin, W. J., Trifonov, J., Petersen-Deitz, K. R., Koltzenburg, M., Basbaum, A. I., and Julius, D. (2000) Impaired nociception and pain sensation in mice lacking the capsaicin receptor. *Science* **288**, 306–313
2. Davis, J. B., Gray, J., Gunthorpe, M. J., Hatcher, J. P., Davey, P. T., Overend, P., Harries, M. H., Latcham, J., Clapham, C., Atkinson, K., Hughes, S. A., Rance, K., Grau, E., Harper, A. J., Pugh, P. L., Rogers, D. C., Bingham, S., Randall, A., and Sheardown, S. A. (2000) Vanilloid receptor-1 is essential for inflammatory thermal hyperalgesia. *Nature* **405**, 183–187
3. Vay, L., Gu, C., and McNaughton, P. A. (2012) The thermo-TRP ion channel family: properties and therapeutic implications. *Br. J. Pharmacol.* **165**, 787–801
4. Sousa-Valente, J., Andreou, A. P., Urban, L., and Nagy, I. (2014) Transient receptor potential ion channels in primary sensory neurons as targets for novel analgesics. *Br. J. Pharmacol.* **171**, 2508–2527
5. Basbaum, A. I., Bautista, D. M., Scherrer, G., and Julius, D. (2009) Cellular and molecular mechanisms of pain. *Cell* **139**, 267–284
6. Díaz-Franulic, I., Caceres-Molina, J., Sepulveda, R. V., Gonzalez-Nilo, F., and Latorre, R. (2016) Structure-driven pharmacology of transient receptor potential channel vanilloid 1. *Mol. Pharmacol.* **90**, 300–308
7. Chen, M. S., Huber, A. B., van der Haar, M. E., Frank, M., Schnell, L., Spillmann, A. A., Christ, F., and Schwab, M. E. (2000) Nogo-A is a myelin-associated neurite outgrowth inhibitor and an antigen for monoclonal antibody IN-1. *Nature* **403**, 434–439
8. GrandPré, T., Nakamura, F., Vartanian, T., and Strittmatter, S. M. (2000) Identification of the Nogo inhibitor of axon regeneration as a Reticulon protein. *Nature* **403**, 439–444
9. Huber, A. B., Weinmann, O., Brösamle, C., Oertle, T., and Schwab, M. E. (2002) Patterns of Nogo mRNA and protein expression in the developing and adult rat and after CNS lesions. *J. Neurosci.* **22**, 3553–3567

10. O'Neill, P., Whalley, K., and Ferretti, P. (2004) Nogo and Nogo-66 receptor in human and chick: implications for development and regeneration. *Dev. Dyn.* **231**, 109–121
11. Caroni, P., and Schwab, M. E. (1988) Antibody against myelin-associated inhibitor of neurite growth neutralizes nonpermissive substrate properties of CNS white matter. *Neuron* **1**, 85–96
12. Vajda, F., Jordi, N., Dalkara, D., Joly, S., Christ, F., Tews, B., Schwab, M. E., and Pernet, V. (2015) Cell type-specific Nogo-A gene ablation promotes axonal regeneration in the injured adult optic nerve. *Cell Death Differ.* **22**, 323–335
13. Mathis, C., Schröter, A., Thallmair, M., and Schwab, M. E. (2010) Nogo-a regulates neural precursor migration in the embryonic mouse cortex. *Cereb. Cortex* **20**, 2380–2390
14. Mingorance-Le Meur, A., Zheng, B., Soriano, E., and del Río, J. A. (2007) Involvement of the myelin-associated inhibitor Nogo-A in early cortical development and neuronal maturation. *Cereb. Cortex* **17**, 2375–2386
15. Wang, J., Chan, C. K., Taylor, J. S., and Chan, S. O. (2008) The growth-inhibitory protein Nogo is involved in midline routing of axons in the mouse optic chiasm. *J. Neurosci. Res.* **86**, 2581–2590
16. Wang, J., Wang, L., Zhao, H., and Chan, S. O. (2010) Localization of an axon growth inhibitory molecule Nogo and its receptor in the spinal cord of mouse embryos. *Brain Res.* **1306**, 8–17
17. Mi, S., Miller, R. H., Lee, X., Scott, M. L., Shulag-Morskaya, S., Shao, Z., Chang, J., Thill, G., Levesque, M., Zhang, M., Hession, C., Sah, D., Trapp, B., He, Z., Jung, V., McCoy, J. M., and Pepinsky, R. B. (2005) LINGO-1 negatively regulates myelination by oligodendrocytes. *Nat. Neurosci.* **8**, 745–751
18. Pernet, V., Joly, S., Christ, F., Dimou, L., and Schwab, M. E. (2008) Nogo-A and myelin-associated glycoprotein differently regulate oligodendrocyte maturation and myelin formation. *J. Neurosci.* **28**, 7435–7444
19. Schwab, M. E. (2010) Functions of Nogo proteins and their receptors in the nervous system. *Nat. Rev. Neurosci.* **11**, 799–811
20. Dodd, D. A., Niederoest, B., Bloechlinger, S., Dupuis, L., Loeffler, J. P., and Schwab, M. E. (2005) Nogo-A, -B, and -C are found on the cell surface and interact together in many different cell types. *J. Biol. Chem.* **280**, 12494–12502
21. Huebner, E. A., Kim, B. G., Duffy, P. J., Brown, R. H., and Strittmatter, S. M. (2011) A multi-domain fragment of Nogo-A protein is a potent inhibitor of cortical axon regeneration via Nogo receptor 1. *J. Biol. Chem.* **286**, 18026–18036
22. Oertle, T., van der Haar, M. E., Bandtlow, C. E., Robeva, A., Burfeind, P., Buss, A., Huber, A. B., Simonen, M., Schnell, L., Brösamle, C., Kaupmann, K., Vallon, R., and Schwab, M. E. (2003) Nogo-A inhibits neurite outgrowth and cell spreading with three discrete regions. *J. Neurosci.* **23**, 5393–5406
23. Joset, A., Dodd, D. A., Halegoua, S., and Schwab, M. E. (2010) Pincher-generated Nogo-A endosomes mediate growth cone collapse and retrograde signaling. *J. Cell Biol.* **188**, 271–285
24. Montani, L., Gerrits, B., Gehrig, P., Kempf, A., Dimou, L., Wollscheid, B., and Schwab, M. E. (2009) Neuronal Nogo-A modulates growth cone motility via Rho-GTP/LIMK1/cofilin in the unlesioned adult nervous system. *J. Biol. Chem.* **284**, 10793–10807
25. Kempf, A., Tews, B., Arzt, M. E., Weinmann, O., Obermair, F. J., Pernet, V., Zagrebelsky, M., Delekat, A., Iobbi, C., Zemmar, A., Ristic, Z., Gullo, M., Spies, P., Dodd, D., Gyax, D., Korte, M., and Schwab, M. E. (2014) The sphingolipid receptor S1PR2 is a receptor for Nogo-a repressing synaptic plasticity [published correction in *PLoS Biol.* 2014, 12, 1001818.] *PLoS Biol.* **12**, e1001763
26. Li, Y., Hu, F., Chen, H. J., Du, Y. J., Xie, Z. Y., Zhang, Y., Wang, J., and Wang, Y. (2014) LIMK-dependent actin polymerization in primary sensory neurons promotes the development of inflammatory heat hyperalgesia in rats. *Sci. Signal.* **7**, ra61
27. Igwe, O. J., and Ning, L. (1994) Regulation of the second-messenger systems in the rat spinal cord during prolonged peripheral inflammation. *Pain* **58**, 63–75
28. Størkson, R. V., Kjørsvik, A., Tjølsen, A., and Hole, K. (1996) Lumbar catheterization of the spinal subarachnoid space in the rat. *J. Neurosci. Methods* **65**, 167–172
29. GrandPré, T., Li, S., and Strittmatter, S. M. (2002) Nogo-66 receptor antagonist peptide promotes axonal regeneration. *Nature* **417**, 547–551
30. Yang, Y. R., He, Y., Zhang, Y., Li, Y., Li, Y., Han, Y., Zhu, H., and Wang, Y. (2007) Activation of cyclin-dependent kinase 5 (Cdk5) in primary sensory and dorsal horn neurons by peripheral inflammation contributes to heat hyperalgesia. *Pain* **127**, 109–120
31. Chaplan, S. R., Bach, F. W., Pogrel, J. W., Chung, J. M., and Yaksh, T. L. (1994) Quantitative assessment of tactile allodynia in the rat paw. *J. Neurosci. Methods* **53**, 55–63
32. Xing, B. M., Yang, Y. R., Du, J. X., Chen, H. J., Qi, C., Huang, Z. H., Zhang, Y., and Wang, Y. (2012) Cyclin-dependent kinase 5 controls TRPV1 membrane trafficking and the heat sensitivity of nociceptors through KIF13B. *J. Neurosci.* **32**, 14709–14721
33. Ahmed, Z., Mazibrada, G., Seabright, R. J., Dent, R. G., Berry, M., and Logan, A. (2006) TACE-induced cleavage of NgR and p75NTR in dorsal root ganglion cultures disinhibits outgrowth and promotes branching of neurites in the presence of inhibitory CNS myelin. *FASEB J.* **20**, 1939–1941
34. Nyatia, E., and Lang, D. M. (2007) Localisation and expression of a myelin associated neurite inhibitor, Nogo-A and its receptor Nogo-receptor by mammalian CNS cells. *Res. Vet. Sci.* **83**, 287–301
35. Ji, R. R., Samad, T. A., Jin, S. X., Schmolli, R., and Woolf, C. J. (2002) p38 MAPK activation by NGF in primary sensory neurons after inflammation increases TRPV1 levels and maintains heat hyperalgesia. *Neuron* **36**, 57–68
36. Zhu, H., Yang, Y., Zhang, H., Han, Y., Li, Y., Zhang, Y., Yin, D., He, Q., Zhao, Z., Blumberg, P. M., Han, J., and Wang, Y. (2008) Interaction between protein kinase D1 and transient receptor potential V1 in primary sensory neurons is involved in heat hypersensitivity. *Pain* **137**, 574–588
37. Ono, Y., Saido, T. C., and Sorimachi, H. (2016) Calpain research for drug discovery: challenges and potential. *Nat. Rev. Drug Discov.* **15**, 854–876
38. Fukiage, C., Azuma, M., Nakamura, Y., Tamada, Y., Nakamura, M., and Shearer, T. R. (1997) SJA6017, a newly synthesized peptide aldehyde inhibitor of calpain: amelioration of cataract in cultured rat lenses. *Biochim. Biophys. Acta* **1361**, 304–312
39. Willi, R., Aloy, E. M., Yee, B. K., Feldon, J., and Schwab, M. E. (2009) Behavioral characterization of mice lacking the neurite outgrowth inhibitor Nogo-A. *Genes Brain Behav.* **8**, 181–192
40. Hu, F., Liu, B. P., Budel, S., Liao, J., Chin, J., Fournier, A., and Strittmatter, S. M. (2005) Nogo-A interacts with the Nogo-66 receptor through multiple sites to create an isoform-selective subnanomolar agonist. *J. Neurosci.* **25**, 5298–5304
41. Cao, T. T., Deacon, H. W., Reczek, D., Bretscher, A., and von Zastrow, M. (1999) A kinase-regulated PDZ-domain interaction controls endocytic sorting of the beta2-adrenergic receptor. *Nature* **401**, 286–290
42. Hough, C., Fukamauchi, F., and Chuang, D. M. (1994) Regulation of beta-adrenergic receptor mRNA in rat C6 glioma cells is sensitive to the state of microtubule assembly. *J. Neurochem.* **62**, 421–430
43. Keenan, C., and Kelleher, D. (1998) Protein kinase C and the cytoskeleton. *Cell. Signal.* **10**, 225–232
44. Dina, O. A., McCarter, G. C., de Coupade, C., and Levine, J. D. (2003) Role of the sensory neuron cytoskeleton in second messenger signaling for inflammatory pain. *Neuron* **39**, 613–624
45. Hsieh, S. H. K., Ferraro, G. B., and Fournier, A. E. (2006) Myelin-associated inhibitors regulate cofilin phosphorylation and neuronal inhibition through LIM kinase and Slingshot phosphatase. *J. Neurosci.* **26**, 1006–1015
46. Iobbi, C., Korte, M., and Zagrebelsky, M. (2017) Nogo-66 restricts synaptic strengthening via Lingo1 and the ROCK2-cofilin pathway to control actin dynamics. *Cereb. Cortex* **27**, 2779–2792
47. Nakanishi, M., Hata, K., Nagayama, T., Sakurai, T., Nishisho, T., Wakabayashi, H., Hiraga, T., Ebisu, S., and Yoneda, T. (2010) Acid activation of Trpv1 leads to an up-regulation of calcitonin gene-related peptide expression in dorsal root ganglion neurons via the CaMK-CREB cascade: a potential mechanism of inflammatory pain. *Mol. Biol. Cell* **21**, 2568–2577
48. Simonen, M., Pedersen, V., Weinmann, O., Schnell, L., Buss, A., Ledermann, B., Christ, F., Sansig, G., van der Putten, H., and Schwab, M. E. (2003) Systemic deletion of the myelin-associated outgrowth inhibitor Nogo-A improves regenerative and plastic responses after spinal cord injury. *Neuron* **38**, 201–211

Received for publication February 28, 2018.

Accepted for publication July 2, 2018.